PRAMANA — journal of physics

Vol. 83, No. 3
September 2014
pp. 395–411

Deuterium–tritium catalytic reaction in fast ignition: Optimum parameters approach

B KHANBABAEI[1], A GHASEMIZAD[1,*] and S KHOSHBINFAR[2]

[1]Physics Department, Faculty of Science, University of Guilan, Rasht, Iran
[2]School of Physics, Damghan University, Damghan, Iran
*Corresponding author. E-mail: ghasemi@guilan.ac.ir

MS received 23 November 2013; revised 14 January 2014; accepted 28 January 2014
DOI: 10.1007/s12043-014-0801-y; ***e*Publication:** 26 August 2014

Abstract. One of the main concerns about the current working on nuclear power reactors is the potential hazard of their radioactive waste. There is hope that this issue will be reduced in next generation nuclear fusion power reactors. Reactors will release nuclear energy through microexplosions that occur in a mixture of hydrogen isotopes of deuterium and tritium. However, there exist radiological hazards due to the accumulation of tritium in the blanket layer. A catalytic fusion reaction of DT_x mixture may stand between DD and an equimolar DT approach in which the fusion process continues with a small amount of tritium seed. In this paper, we investigate the possibility of DT_x reaction in the fast ignition (FI) scheme. The kinematic study of the main mechanism of the energy gain–loss term, which may disturb the ignition and burn process, was performed in FI and the optimum values of precompressed fuel and proton beam driver were derived. The recommended values of fuel parameters are: areal density $\rho R \geq 5\,\mathrm{g}\cdot\mathrm{cm}^{-2}$ and initial tritium fraction $x \leq 0.025$. For the proton beam, the corresponding optimum interval values are proton average energy $3 \leq E_\mathrm{p} \leq 10$ MeV, pulse duration $5 \leq t_\mathrm{p} \leq 15$ ps and power $5 \leq W_\mathrm{p} \leq 12 \times 10^{22}$ ($\mathrm{keV}\cdot\mathrm{cm}^3\cdot\mathrm{ps}^{-1}$). It was proved that under the above conditions, a fast ignition DT_x reaction stays in the catalytic regime.

Keywords. Fast ignition; catalytic regime; ion beam; tritium breeding; burn dynamics.

PACS Nos 52.57.Kk; 52.40.Mj; 52.58.Ei

1. Introduction

Application of hydrogen isotopes as a potential fuel for next generation nuclear reactors lies at the heart of current nuclear fusion researches around the world [1]. However, pure deuterium–deuterium (DD) combination is sensitive to the condition of overdense plasma and to achieve a relatively higher temperature (∼100 keV), more energy and stronger external drivers are needed [2]. In competition with DD fuels, deuterium–tritium (DT), due to its higher relative fusion cross-sections at lower plasma temperature (about 10 keV), is considered to be a more favourable option as the first candidate

of next generation commercial fusion reactors. It, however, has potential radiological hazards associated with the accumulation of tritium in the blanket layer of the reactor core [3].

One of the recent alternative scenarios which was proposed by Eliezer clearly focusses on deuterium fuel with a small amount of tritium impurity. The obvious advantage of this method is the removal of the blanket layer from reactor design [4]. The addition of a small amount of tritium seeds in pure deuterium fuel will reduce the ignition temperature of the DT_x mixture (x represents the initial tritium to deuterium ratio) to a temperature between that of pure DD and DT fuels. After this, a few studies inspired by the method tried to find optimum conditions for advanced fuels. They all studied various aspects of the ignition condition, burning and its corresponding fuel energy gains in the framework of the standard model of inertial confinement fusion (ICF), viz., the central spark ignition (CSI) [5].

Currently, fast ignition (FI) schemes in ICF are proposed as an interesting shortcut to bypass difficulties such as Rayleigh–Taylor instability [6]. This method is based on a two-step approach. First, a high-power external driver such as a laser or an ion beam is used to illuminate the target surface to maintain a precompressed condition. In the second step, a more powerful, short time beam is used to form a hot spot inside the illuminated area. The main characteristic of the latter is the 2–5 ps time interval relative to 10–30 ps of the first one [7]. Recently, further studies have been directed to the application of light/heavy ion drivers due to their higher potential for future reactors such as higher repetition rate [8].

In this paper, considerable attempt has been made to bring modern charged particle energy loss mechanisms in fusion plasma, taking into account the large-angle Coulomb scattering, quantum effects, collective effects in plasma, and nuclear elastic scattering contributions, into the study of the ignition and burn dynamics in a fast ignition framework. We have also incorporated the main features of the external driver, like pulse shape, its duration, power and intensity. Under the above conditions, the optimized range of different parameters and initial tritium fraction has been derived and discussed with reference to previous studies.

2. Kinematic considerations

The fast ignition scheme has been considered as a robust approach to inertial confinement fusion (ICF) which differs significantly from the conventional central-hot-spot ignition ICF. It has a two stage process, first of which begins with the precompressed state of the fuel achieved through illumination by a long-pulse (ns) driver (laser beams, X-rays) which is then ignited by a short-pulse (ps) laser (particles) beam [9]. The technological advantage of this method is the reduced sensitivity of the compression process to the growth of the Rayleigh–Taylor instability. This is a significant milestone as compared to the standard approach which suffers from hydrodynamical instabilities in the implosion phase. We also expect to achieve a higher energy gain for the same driver input energy [10].

In the original idea of fast ignition, relativistic electrons produced in the course of laser–target interaction are responsible to form an off-centre hot spot by local energy

deposition. A few years later, it gained more acceptance and innovative target designs like cone-guided targets were proposed. Long range and focussing of hot electrons are issues that motivate researchers to assess the reliability of ion beams [11]. Protons are always considered the most important light ion beams due to their highest charge-to-mass ratio; they are accelerated most efficiently to the highest energies. Extensive simulation and experiments in recent years have confirmed this idea [12]. The spatio-temporal nature of energy deposition patterns is basically of great importance in fast ignition scheme. From a practical point of view, generating a quasimonoenergetic distribution of particle beams has satisfied most of the requirements of local energy deposition and beam focussing issues [13]. The energy of the particles as well as their intensity has a direct effect on the size and shape of the produced hot spot and hence should be controlled carefully. Atzeni and his coworkers showed that optimum range of charged particles in a precompressed target lies between $0.15 \leq \rho R \leq 1.2\ \mathrm{g \cdot cm^{-2}}$ [14]. They have also shown that while the beam spot and ion penetration depth remain much smaller than the target radius, the corresponding results are nearly independent of precompressed fuel dimension [14]. The areal density of the precompressed fuel influences the expected amount of energy released in nuclear fusion microexplosion. So, there should be enough space to propagate the burning waves in a larger fraction of the fuel. It is common in ICF numerical simulations to assume an equimolar DT fuel in precompressed stage with density as large as 1000 solid densities, a temperature interval of 1–4 keV and a corresponding areal density of 1.5–5 $\mathrm{g \cdot cm^{-2}}$ [15]. These values are somewhat sensitive to the composition of the precompressed fuel. Recently, for pure deuterium fuel, with the addition of a small amount of tritium impurity, Atzeni *et al* adapted the values of density $500 \leq \rho \leq 1000\ \mathrm{g \cdot cm^{-3}}$ and areal density of $5 \leq \rho R \leq 15\ \mathrm{g \cdot cm^{-2}}$ in their studies [16,17].

In previous studies of DT_x catalytic regime, the following three important assumptions were made: firstly, the central spark ignition model governed the whole process and secondly, the hot spot region was formed before and finally the ignition process assumed volumetrically [4]. In the current study, we have tried to include the effects of catalytic regime in fast ignition scheme, driver particles energy, intensity and pulse duration, regardless of the production mechanism of these particles. So, we have also assumed pure deuterium fuel with a small amount of tritium seed, a uniform density $\rho = 500\ \mathrm{g \cdot cm^{-3}}$, the same initial electron and ion temperatures of $T(T_\mathrm{i} = T_\mathrm{e}) = 4$ keV and irradiated by beams of protons of density $\rho R = 10\ \mathrm{g \cdot cm^{-2}}$ as our initial configuration. This is depicted schematically in figure 1.

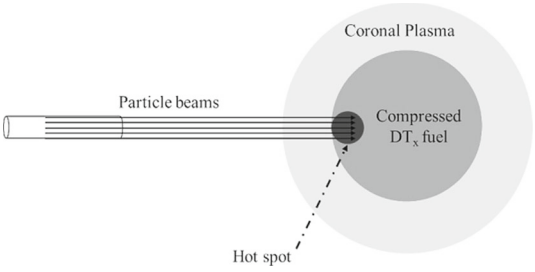

Figure 1. The fast ignition scheme, launched by incident proton beam.

To study ignition condition and subsequent burn phase, we must take into account the energy gain and loss mechanisms. The contribution to the gain processes comes from external driver ions, plasma accelerated ions and to a small extent, the neutrons produced by DT reaction. In contrast, for the loss processes, electron's bremsstrahlung radiation, inverse Compton scattering and plasma expansion are the main mechanisms of energy dissipation. The following nuclear fusion reactions occur predominantly in the fuel pellet:

$$^{2}_{1}\mathrm{D} + {}^{2}_{1}\mathrm{D} \rightarrow {}^{1}_{0}\mathrm{n} + {}^{3}_{2}\mathrm{He} + 3269\ \mathrm{keV}, \tag{1}$$

$$^{2}_{1}\mathrm{D} + {}^{2}_{1}\mathrm{D} \rightarrow {}^{1}_{1}\mathrm{p} + {}^{3}_{1}\mathrm{T} + 4033\ \mathrm{keV}, \tag{2}$$

$$^{2}_{1}\mathrm{D} + {}^{3}_{1}\mathrm{T} \rightarrow {}^{1}_{0}\mathrm{n} + {}^{4}_{2}\mathrm{He} + 17589\ \mathrm{keV}, \tag{3}$$

$$^{2}_{1}\mathrm{D} + {}^{3}_{2}\mathrm{He} \rightarrow {}^{1}_{1}\mathrm{p} + {}^{4}_{2}\mathrm{He} + 18353\ \mathrm{keV}, \tag{4}$$

where in eqs (1) and (2), pure DD reaction channels have equal probability. We then study the rates of produced and consumed particles inside the fuel pellet by taking into account the above-mentioned mechanisms. At any moment, the total number of particles of the species, $k(N_k)$, can be calculated by the following equation;

$$V\frac{\mathrm{d}N_k}{\mathrm{d}t} = \sum_{j=1}^{4} c_k^j N_{j(1)} N_{j(2)} \langle\sigma\nu\rangle_j\,, \tag{5}$$

where N_js denote the number of particles per unit volume of the fuel, $\langle\sigma\nu\rangle_j$ is the averaged Maxwellian reaction rate and c_k^j stands for the number of particles of species k formed/destroyed in the reaction j. The total number of six species considered in our calculation are D, ^{3}He, T, proton, ^{4}He and neutron particles. As we have plasma at two temperatures, we write the energy balance equations for ions and electrons separately as follows:

$$\begin{aligned} V\frac{3}{2}\frac{\mathrm{d}}{\mathrm{d}t}(N_\mathrm{i}T_\mathrm{i}) = {} & \sum_{j=1}^{4}\sum_{k=1}^{6}(1-\eta_k^j) f_k^j w_k^j E_j N_{j(1)} N_{j(2)} \langle\sigma\nu\rangle \\ & + \eta_\mathrm{p} W_\mathrm{p} - P_\mathrm{ie} - N_\mathrm{i}T_\mathrm{i} 4\pi R^2(t) C_\mathrm{s}, \end{aligned} \tag{6}$$

$$\begin{aligned} V\frac{3}{2}\frac{\mathrm{d}}{\mathrm{d}t}(N_\mathrm{e}T_\mathrm{e}) = {} & \sum_{j=1}^{4}\sum_{k=1}^{6}((1-\eta_k^j)(1-f_k^j) w_k^j E_j N_{j(1)} N_{j(2)} \langle\sigma\nu\rangle \\ & + (1-\eta_\mathrm{p}) W_\mathrm{p} + P_\mathrm{ie} - P_\mathrm{B} - P_\mathrm{C} V - N_\mathrm{i}T_\mathrm{i} 4\pi R^2(t) C_\mathrm{s}), \end{aligned} \tag{7}$$

where T_i, E_j, η_p, w_k^j, η_k^j, f_k^j and $R(t)$ are ion temperature, energy yield of reaction j, fraction of the beam energy deposited in the ions, fraction of E_j carried by the product k, energy leakage probability of produced ions, fraction of the energy of the product k formed in the reaction j that is deposited into the plasma ions, and the fuel radius, respectively. Moreover, C_s is the speed of sound, T_e is the electron temperature, P_B is the

bremsstrahlung radiation term and P_C is the inverse Compton scattering term. The total number of ions, N_i, is

$$N_i = \sum_{k=2}^{6} N_k, \tag{8}$$

where for neutrons, k is equal to 1 and for the rest of them it varies from 2 to 6. When the plasma has a temperature of a few keV, the charged particles may lose part of their energies through light emission while being decelerated by plasma ions. Because of the higher mobility of electrons as compared to ions, this radiation loss is more important for electrons. The energy loss term, P_B, is given by [18]:

$$P_B\left(\text{keV cm}^3\ \text{s}^{-1}\right) = 2.94 \times 10^{-15} \sum_{k=1}^{6} N_e N_k Z_k^2 \left(\sqrt{T_e} + \frac{2T_e^{3/2}}{m_{0e}c^2}\right), \tag{9}$$

where $E_0 = m_{0e}c^2$ is the rest energy of plasma electrons.

Because of the spatiotemporal variation of plasma temperature and density in the fuel pellet during the burning phase, its optical transparency will also change. For optically thick plasma, bremsstrahlung radiation photons have a shorter mean free path than the fuel size. Because of this, they act as a photon gas in thermal equilibrium condition. In this case, the inverse Compton effects can significantly reduce the electron temperature and correspondingly raise the radiation temperature. But, in optically thin plasma, photons produced by the bremsstrahlung emission can leave the plasma medium before the equilibrium is established, and do not have any considerable interaction with plasma electrons. In the burn phase, plasma rapidly switches from the optically thick to thin mode. Therefore, the following equation is used to include the inverse Compton scattering contribution [19]:

$$P_C\left(\text{keV s}^{-1}\right) = 1.67\pi r_e^2 E_r N_e c \left(\frac{\Delta T_{e,r}}{m_{0e}c^2}\right), \tag{10}$$

where r_e is Bohr radius of the electrons, N_e is the total number of plasma electrons, $\Delta T_{e,r}$ stands for temperature gradient between electrons and photons and E_r is the total radiation energy density. In burning plasma, electrons due to inverse Compton scattering and bremsstrahlung radiation will receive lower temperatures than ions. This temperature difference causes energy transfer from ions to electrons which can be expressed as below [20]:

$$P_{ie}\left(\text{keV cm}^3\ \text{s}^{-1}\right) = 1.69 \times 10^{-13} \sum_{k=1}^{6} N_e \frac{\ln\Lambda_{ek} Z_k^2 N_k \Delta T_{i,e}}{m_k T_e^{3/2}}, \tag{11}$$

where $\Delta T_{e,i}$ is the temperature difference between electrons and ions, $\ln \Lambda_{ek}$ is the electron Coulomb logarithm, m_k and Z_k are the mass number and the charge of nuclei k respectively.

Precompressed fuel has uniform density and isobaric condition. In this case, the thermodynamic pressure is obtained from the following relation:

$$P = \frac{1}{V}\left(N_i T_i + N_e T_e\right). \tag{12}$$

Time evolution of the radius of the fuel pellets is

$$R(t) = F(t)c_s(t). \tag{13}$$

In the above equation, $F(t)$ is a function of the fuel burn-up fraction [21].

2.1 *Energy loss mechanisms in hot plasmas*

The key to study the ignition condition in the fast ignition method is a proper knowledge of energy loss mechanisms, which always try to dissipate heat to plasma boundaries. So, detailed observations of different contributions that have effects on the penetration depth and hot-spot state are required. So, we have to account for the competition of these components at different states of the plasma during its evolution. As mentioned before, the most important energy deposition mechanisms can be categorized as Coulomb scattering, nuclear elastic scattering and neutrons.

2.2 *Coulomb scattering*

In the case of low-density, high-temperature plasmas, Coulomb interactions can be approximated as small angle binary collisions [22]. However, large-angle Coulomb scattering and collective plasma effects need to be included at high densities [23]. These parameters increase the stopping power of the incident (or produced) charged particles transport in fusion plasmas. The lower particles range in plasma causes a smaller hot spot size. So, we should not only take into account primary incident particles transport inside the colder precompressed fuel, but also do the same for secondary charged particles formed in fusion reactions and plasma accelerated particles. This complicates the Coulomb scattering process. Li and Petrasso derived an analytical expression for the charged particle stopping power by the assumption of including the contribution of large angle scattering in the Fokker–Plank equation [24].

The stopping power of the incident charged particle projectile t with mass m_t to the plasma particles of species f with mass m_f or, equivalently, the energy gain of the plasma particles f brought about by the projectile t moving through the plasma with velocity v_t, is defined as

$$\frac{\mathrm{d}E^{t/f}}{\mathrm{d}x} = -\frac{(Z_t e)^2}{v_t^2}\frac{4\pi n_f \left(Z_f e\right)^2}{m_f} \times \left\{G\left(\chi^{t/f}\right)\ln\Lambda_b + \Theta\left(\chi^{t/f}\right)\ln\left[1.123\left(\chi^{t/f}\right)^{1/2}\right]\right\}, \tag{14}$$

where function G is defined as

$$G\left(\chi^{t/f}\right) = \mu\left(\chi^{t/f}\right) - \frac{m_f}{m_t}\left\{\frac{\mathrm{d}\mu\left(\chi^{t/f}\right)}{\mathrm{d}\chi^{t/f}} - \frac{1}{\ln\Lambda_b}\left[\mu(\chi^{t/f}) + \frac{\mathrm{d}\mu\left(\chi^{t/f}\right)}{\mathrm{d}\chi^{t/f}}\right]\right\}, \tag{15}$$

where

$$\mu\left(\chi^{t/f}\right) = \frac{2}{\sqrt{\pi}}\int_0^{x^{t/f}} \mathrm{e}^{-\xi}\sqrt{\xi}\mathrm{d}\xi \tag{16}$$

and $\Theta\left(x^{t/f}\right)$ is a step function whose value is 0 for $x^{t/f} \leq 1$ and 1 for $x^{t/f} > 1$.

2.3 *Nuclear elastic scattering*

The weight of nuclear elastic scattering (NES) is more important in the calculation of the stopping power of high-temperature plasmas. Deviation of velocity distribution functions of fuel particles due to nuclear elastic scattering results in enhancing the fusion cross-section, and consequently has an influence on the nuclear fusion reaction rate [25]. It will change the energy spectrum of particles from normal distribution especially at higher energies. So, the contributions of these highly energetic particles are very important in fusion plasma heating. Strictly speaking, nuclear elastic scattering accelerates the process of stopping power and lowers the range of more energetic ions [26]. The averaged energy loss due to NES can be estimated [27] as

$$\left(\frac{\mathrm{d}E_t}{\mathrm{d}x}\right)^{\mathrm{NES}} = -4\pi n_f E_t \frac{m_t m_f}{\left(m_t + m_f\right)^2} \int_{-1}^{1} \left(\frac{\mathrm{d}\sigma}{\mathrm{d}\Omega}\right)(1-\mu)\,\mathrm{d}\mu, \tag{17}$$

where $\mathrm{d}\sigma/\mathrm{d}\Omega$ represents the differential NES cross-section and is suggested as the exact polynomial expansion [28];

$$\frac{\mathrm{d}\sigma}{\mathrm{d}\Omega} = -\frac{2\eta}{1-\mu}\mathrm{Re}\left[\exp\left(i\eta\ln\left(\frac{1-\mu}{2}\right)\right)\sum_{0}^{l_{\max}}\frac{2l+1}{2}a_l P_l(\mu)\right] + \sum_{0}^{2l_{\max}}\frac{2l+1}{2}b_l P_l(\mu), \tag{18}$$

where η is the Coulomb parameter and $l_{\max}$ is the highest partial wave mode that participates in nuclear scattering. The complex number expansion coefficients a_l and real coefficients b_l are energy dependent and interrelated in complicated ways that can only be imposed by a unitary parametrization of the collision matrix (such as the R-matrix or phase shifts). Using eqs (14) and (18), the fraction of energy deposited to the plasma ions can be calculated as follows:

$$f_k^j = \frac{1}{\omega_k^j E_j - \frac{3}{2}T_{\mathrm{i}}}\int_{\frac{3}{2}T_{\mathrm{i}}}^{\omega_k^j E_j}\frac{(\mathrm{d}E/\mathrm{d}x)_{\mathrm{i}}^{(c)} + (\mathrm{d}E/\mathrm{d}x)_{\mathrm{i}}^{(\mathrm{NES})}}{(\mathrm{d}E/\mathrm{d}x)_{\mathrm{e}}^{(c)} + (\mathrm{d}E/\mathrm{d}x)_{\mathrm{i}}^{(c)} + (\mathrm{d}E/\mathrm{d}x)_{\mathrm{i}}^{(\mathrm{NES})}}\mathrm{d}E. \tag{19}$$

2.4 *Neutron energy deposition*

Neutrons are neutral particles which are produced in the fusion reaction of DT fuel. They do not enter into the energy loss process like charged particles. Most of them escape from the target boundaries and can only be trapped in some outer layers. Researchers showed that when the areal density of fusion fuel is about 5 g · cm^{-2} and more, then the probability of neutron interaction with background plasma ions will be more [29]. So, neutrons inject a part of their energies into the plasma medium for DD and DT reactions [30]. For 14.1 MeV neutrons produced in DT reaction, the fraction of the deposited energy is obtained by

$$f_{\mathrm{n}} = \frac{\rho R}{H_{\mathrm{n}} + \rho R}, \tag{20}$$

where H_{n} is the burn parameter which should be evaluated at an appropriately averaged burn temperature T.

3. Results and discussion

Now, based on the above-mentioned mechanisms of energy gain–loss competitions, we have investigated the optimum conditions for the catalytic regime of deuterium fuel with tritium seed. It has been shown that in high-temperature plasma, it is better to take into account the thermal motion of plasma components. This may appear as a correction term for the position of particles for collisional interactions, fuel parameters and energy gain results. Hence, we have also included the effect of the shift of the centre-of-mass in binary collisions [31]. In inertial confinement fusion, target energy gain is defined as yield energy to invested ratio:

$$\text{Gain} = \frac{E_{\text{fusion}}^{\text{tot}}}{E_{\text{com}} + E_{\text{ign}}}, \tag{21}$$

where the total energy is defined as

$$E_{\text{fus}}^{\text{tot}} = \int_0^{\infty} \mathrm{d}t \sum_{j=1}^{4} E_j \langle \sigma v \rangle_j N_{j(1)} N_{j(2)}. \tag{22}$$

E_{ign} is determined by the power of incident beam and E_{com} in the denominator of eq. (21) is written as

$$E_{\text{com}} = \frac{3}{2} \left[N_{\text{e}}(0) T_{\text{e}}(0) + N_{\text{i}}(0) T_{\text{i}}(0) \right]. \tag{23}$$

Furthermore, to investigate the catalytic state of tritium in the fusion fuel, the quantity of tritium breeding ratio is defined as below:

$$\gamma_{\text{br}} = \frac{N_{\text{T}}\,(t = \infty)}{N_{\text{T}}\,(t = 0)} \tag{24}$$

which is the ratio of tritium in the burning state to its initial content. The tritium in the fuel will be in the catalytic mode, when the parameter $\gamma \geq 1$. Fuel burn fraction is defined as

$$f_{\text{b}} = \frac{N_{\text{D,initial}} - N_{\text{D,final}}}{N_{\text{D,initial}}}, \tag{25}$$

where $N_{\text{D,initial}}$ and $N_{\text{D,final}}$ are the total number of deuterons in the pellet initially and the number left in the pellet after burn, respectively.

Major factors which act on the level of internal tritium breeding will be discussed in two parts; driver parameters and fuel state.

3.1 *Driver characters*

It is assumed that in the initial state, we have a precompressed DT_x fuel pellet (tritium fraction x, in the pre-compressed fuel is uniformly distributed) with state parameters of density $\rho = 500\ \text{g}\cdot\text{cm}^{-3}$, $\rho R = 10\ \text{g}\cdot\text{cm}^{-2}$ and initial temperature $T_{\text{i}} = T_{\text{e}} = 4$ keV. These values are derived from detailed numerical simulation and lab experiments [16,17]. As our initial guess of the tritium fraction, the subscript x in DT_x, we chose the value proposed by Eliezer team which is $x = 0.0112$ [30].

In figure 2, the range of incident beam against plasma temperature for different energies of proton is shown. The fuel configuration is assumed to be in a state of mass density $\rho = 500\ \mathrm{g \cdot cm^{-3}}$ and $x = 0.0112$. These calculations have been performed by employing the stopping power model by Li and Petrasso. For the common drivers used in ICF, Atzeni showed that the range interval of the incident ion beam is 0.15–1.2 $\mathrm{g \cdot cm^{-2}}$ [14]. For the particle range of interest and precompressed fuel temperatures, we observe that the proper choice of proton beam energy would fall in $3 \leq E_\mathrm{p} \leq 10$ MeV.

In figure 3a, time evolution of tritium breeding ratio for three different average particle energies 3, 8 and 15 MeV is shown. The profile of proton energy spectrum adopted is quasimonoenergetic. The precompressed fuel is in a state with density $\rho = 500\ \mathrm{g \cdot cm^{-3}}$, $\rho R = 10\ \mathrm{g \cdot cm^2}$, the initial temperature $T_\mathrm{i} = T_\mathrm{e} = 4$ keV and tritium fraction $x = 0.0112$, and is irradiated by the proton beam of 8×10^{22} ($\mathrm{keV \cdot cm^3 \cdot ps^{-1}}$) power during 8 ps box shape pulse duration. Here, we can see that the behaviour of tritium breeding ratio for various proton beams appears to have a relatively similar evolution. In the first ps, the consumption regime governs the start of the fusion reaction. The minimum ratio happens around 7 ps. After that, the ratio rapidly speeds up monotonically and around 14 ps crosses the break-even line. It then reaches its highest value around 47 ps. This pattern is maintained for almost the full range of chosen energies and tends to slightly relax in the next time intervals. Moreover, it is clearly observed that the breeding ratio is almost insensitive to proton energies especially at higher driver energies. In figure 3b, the corresponding fuel burn fraction for different proton energies is shown. It shows a linear variation below 9 MeV energy. In this case, the burn fraction falls between 0.375 and 0.385 for the whole proton energy interval.

To study the tritium breeding ratio of precompressed fuel, we must not only consider particle intensities, but also should, in parallel, control the energy transferred to the target. Here, this may be examined by the power of the proton beams. In figure 4a, the corresponding tritium breeding ratio is shown for three different values of proton beam

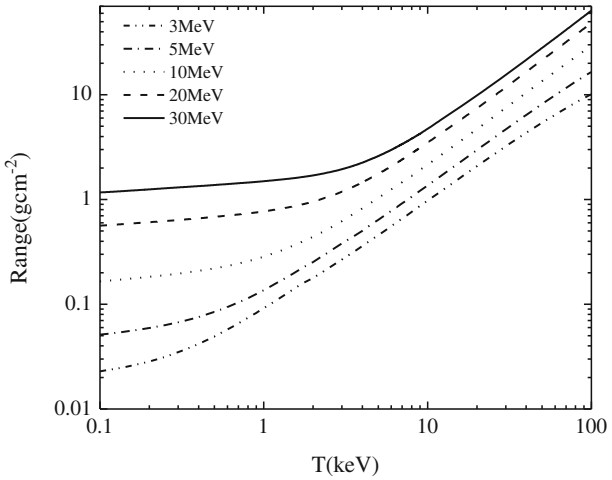

Figure 2. Calculated range, R, of protons beam vs. plasma temperature T.

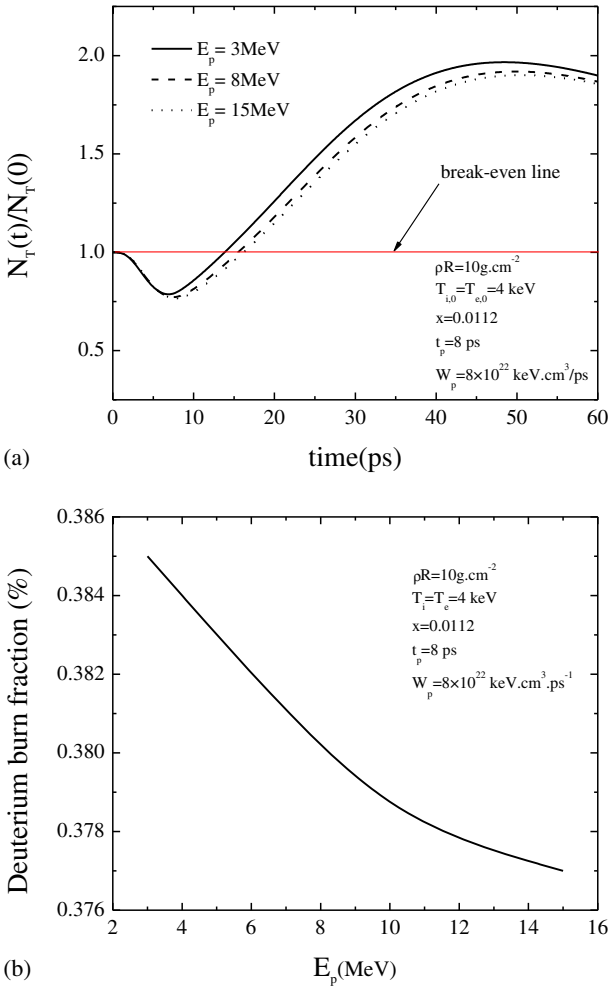

Figure 3. (**a**) Time evolution of tritium breeding ratio and (**b**) tritium burn fraction for different proton energies.

power ($\times 10^{22}$ keV $\cdot$ cm^3 $\cdot$ ps^{-1}). The remaining plasma state parameters are adopted as in figure 3 except that now the proton beam has 3 MeV energy. For the lowest energy, the breeding ratio will remain in the tritium consuming regime. It, however, reappears in the production process for the other two energies. The values cross the break-even line in a few ps and increase continuously and the position of crossing point is shifted to the intial time of the fuel burning process. Further, an asymptotical behaviour for the boosted driver power is also seen. Fuel burn fractions vary as shown in figure 4b for different values of total pulse power. As can be seen, boosting driver power directly increases the fuel burn fraction. This sharp growth continues up to the value of around 8×10^{22} (keV $\cdot$ cm^3 $\cdot$ ps^{-1}) after which the curve is slightly bent down smoothly. Hence, for the power values more than 12×10^{22} (keV $\cdot$ cm^3 $\cdot$ ps^{-1}), no significant change is observed.

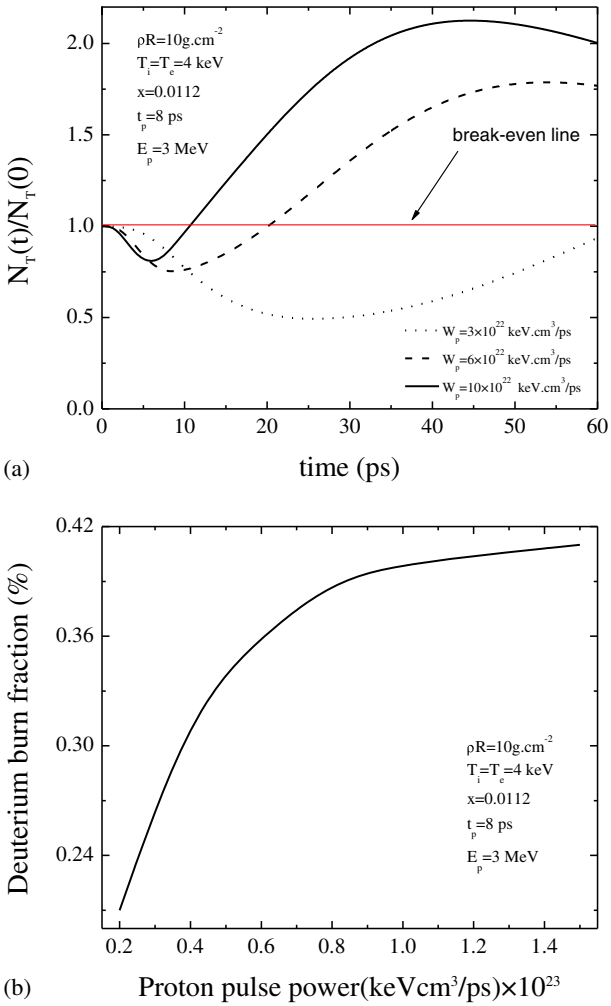

Figure 4. (**a**) Variation of tritium breeding ratio with change in beam power and (**b**) the corresponding fuel burn fraction in terms of proton power.

Having examined the driver parameters, we now focus on the pulse duration time interval, t_p. Pulsing interval determines the number of particles that reach the target with definite energies. To begin with, larger target bombardment speeds up fusion reaction rate which in turn results in the growth of the tritium ions population in fuel plasma. In figure 5a, these results can be easily observed at all pulse durations.

For the shortest pulse duration, $t_p = 3$ ps, the break-even condition for tritium breeding is satisfied around 37 ps, which, in comparison to the plasma hydrodynamical time-scale, 70 ps, will be a somewhat fragile situation. A better choice would be 5 ps pulse duration where the corresponding condition is met around 22 ps. Obviously, a longer pulse duration will result in reaching the break-even point quicker. At equal intervals, from

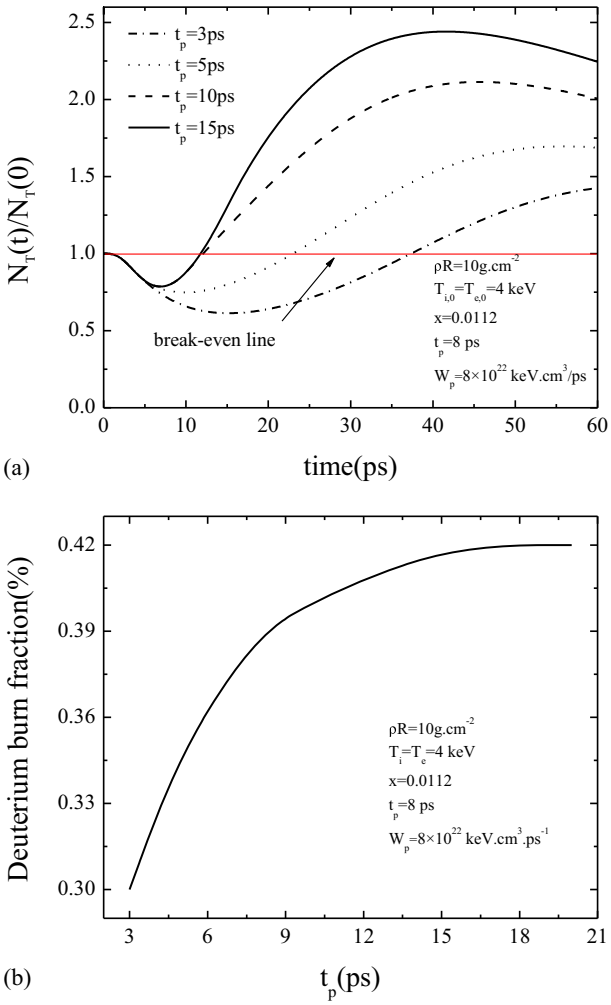

Figure 5. (**a**) Tritium breeding ratio evolution as a function of driver pulse duration and (**b**) the corresponding fuel burn fraction.

5 ps to 15 ps, we can see that the variation of tritium breeding ratio loses its sensitivity to pulse duration and reaches an asymptotic value. This could be seen for pulse durations more than these values. In the latter case, the breeding ratio reduces quickly at time greater than 50 ps which destroys our desired conditions.

3.2 *Precompressed fuel state*

The second factor which may affect the tritium breeding ratio arises from the state of the precompressed fuel. To investigate the effect of initial surface density of the fuel on internal tritium breeding, we consider the fuel pellet parameters at the moment of

the burning process with an initial temperature $T_i = T_e = 4$ keV and tritium fraction $x = 0.0112$, i.e., irradiated by a proton beam of 3 MeV energy with a total power of 8×10^{22} (keV$\cdot$ cm$^3\cdot$ ps^{-1}) and 8 ps pulse duration. The resulting variation in the tritium breeding ratio for different values of fuel areal density is shown in figure 6a.

Based on this calculation, the breeding ratio valley would be deeper for higher values of areal densities. They all experience a transient phase in a few ps and then grow consciously until they reach a maximum tritium inventory. At this point, with a high tritium reservoir, we expect to observe a clear increase in reaction rate where most of the tritium is consumed. Later on, we shall see a decrease on the breeding ratio curves. Out of all the values, an areal density between 5 and 10 g$\cdot$cm^{-2} would be a proper choice as

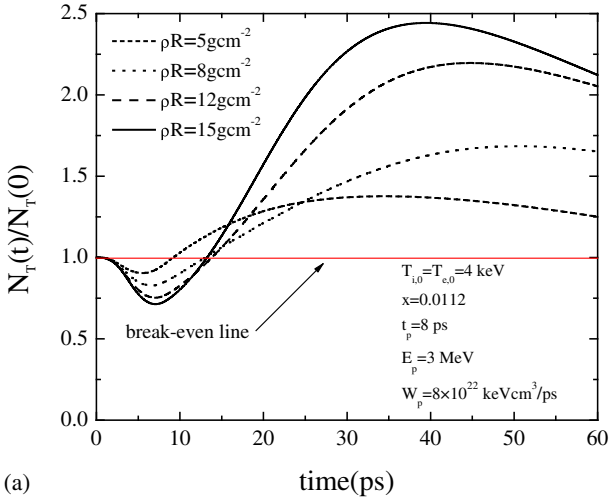

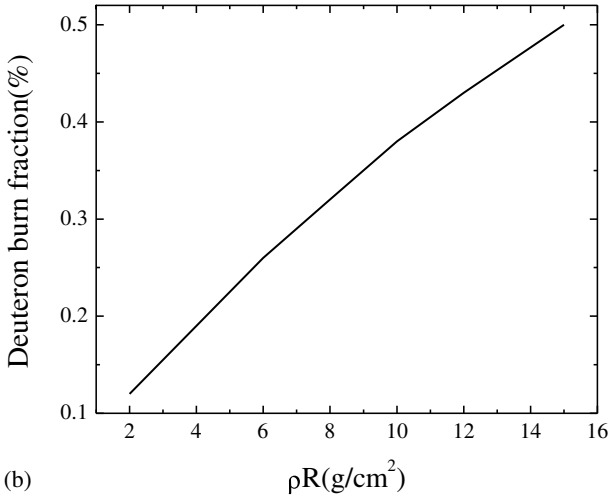

Figure 6. (**a**) Variation in tritium breeding ratio for different values of fuel areal density and (**b**) the corresponding fuel burn fraction.

both these values tend to a slow varying function in time. For initial areal density greater than 15 $g \cdot cm^{-2}$, the tritium breeding ratio function shows an asymptotical picture and will be less sensitive to its changes. The variation of the fuel burn fraction, depending on the fuel areal density, is shown in figure 6b. According to this figure, variations of initial fuel areal density have a large impact on the fuel burn fraction. For areal densities lower than 5 $g \cdot cm^{-2}$, the corresponding fuel burn fraction has a value of less than 20%, which is unacceptable.

The time variation of internal tritium breeding is shown in figure 7a in terms of the tritium initial fraction, x, in the precompressed DT_x fuel plasma. As in previous cases, the initial fuel parameters have been chosen, such that we have DT_x fuel plasma with density

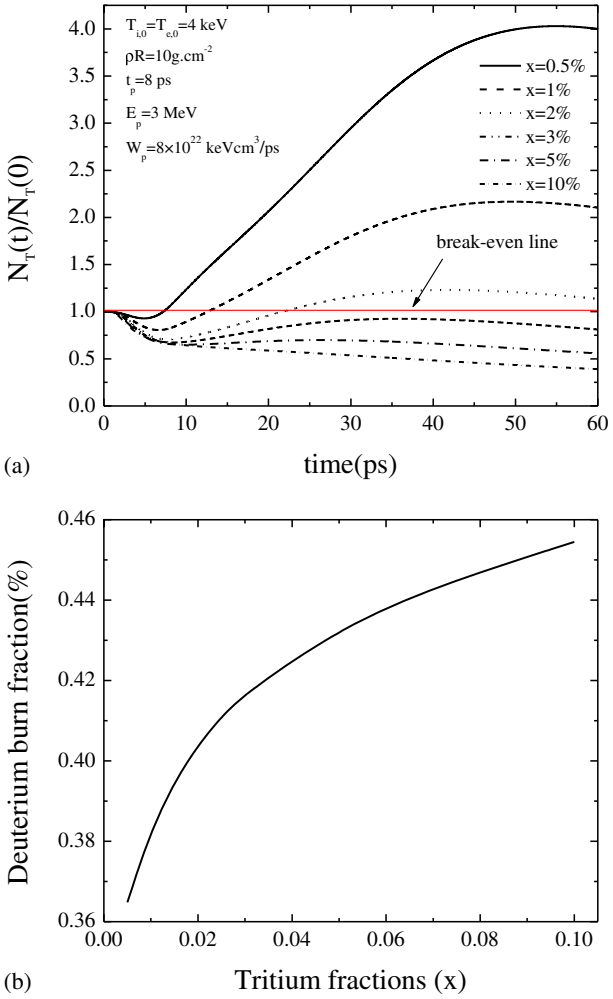

Figure 7. (**a**) Variation of tritium breeding ratio as a function of initial tritium seed fraction and (**b**) the corresponding fuel burn fraction.

$\rho = 500\ \mathrm{g \cdot cm^{-3}}$, $\rho R = 10\ \mathrm{g \cdot cm^{-2}}$ and initial temperature $T_\mathrm{i} = T_\mathrm{e} = 4$ keV, that is irradiated by a proton beam of 3 MeV energy, with a total power of 8×10^{22} ($\mathrm{keV \cdot cm^3 \cdot ps^{-1}}$) and 8 ps pulse duration. As can be seen here, tritium breeding ratios are strongly sensitive to the initial fraction where for values above 2%, the fusion system enters a regime of full consumption and exhibits an asymptotic behaviour for larger tritium fractions. For the initial tritium fraction attained at 2.5%, the breeding ratio shows a grazing curve. It oscillates around the break-even line and will reach equilibrium at 28 ps. Hence, the recommended range of initial tritium fraction would be between 1 and 2%, which is close to the upper limit. So, our calculations show that unit tritium ratio is maintained between 12 and 22 ps and beyond 30 ps, the equilibrium condition is established. It seems that a catalytic regime requirement will be satisfied at this condition. The corresponding fuel

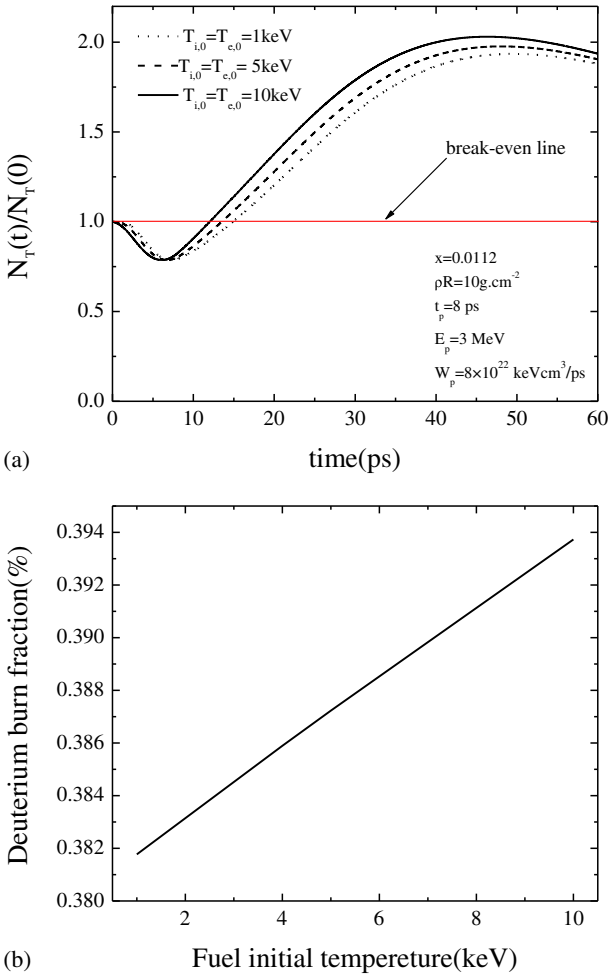

Figure 8. (**a**) Variation of tritium breeding ratio as a function of plasma temperature and (**b**) the corresponding fuel burn fraction.

Table 1. Proper range of fuel and driver characteristic at the precompressed condition.

Fuel pellet		Proton beam parameter	
Areal density	$\rho R \geq 5\ \mathrm{g \cdot cm^{-2}}$	Proton energy	$3 \leq E_\mathrm{p} \leq 10$ MeV
Tritium fraction	$x \leq 0.025$	Pulse duration	$5 \leq t_\mathrm{p} \leq 15$ ps
Temperature of plasma	$1 \leq T_{\mathrm{i},0} = T_{\mathrm{e},0} \leq 10$ keV	Proton beam power	$5 \leq W_\mathrm{p} \leq 12 \times 10^{22}$ $(\mathrm{keV \cdot cm^3 \cdot ps^{-1}})$

burn fraction as a function of tritium fraction is shown in figure 7b. Here, the fuel burn fraction follows a growing curve with initial fraction of tritium. It confirms our recent interpretation of figure 7a about the critical role of the initial tritium seed. Burn fraction growth rate is suppressed and is close to 1%. Therefore, in order to achieve higher fusion gain, we have to constrain the limits of tritium fraction to around its optimal value for the target design.

Li-Petrasso showed that the energy deposition level and distribution are strongly influenced by the plasma temperature such that the ratio of transferred energy to plasma ions and electrons vary with the fuel plasma temperature. In the literature, the value of precompressed fuel temperature is 5 keV which corresponds to the medium temperature condition. In figure 8a, time evolution of tritium breeding in DT_x fuel pellet, for three initial temperatures is given. Here, fuel pellet with density $\rho = 500\ \mathrm{g \cdot cm^{-3}}$, $\rho R = 10\ \mathrm{g \cdot cm^{-2}}$ and tritium fraction $x = 0.0112$, was irradiated by a proton beam of 3 MeV energy with a total power of 8×10^{22} $(\mathrm{keV \cdot cm^3 \cdot ps^{-1}})$ and 8 ps pulse duration. Results show that with increase in temperature of the precompressed fuel in the range of 1–10 keV, tritium breeding content quickly attained its maximum value in a time interval of 12–15 ps. Beyond this, the breeding ratio goes up and reaches its maximum around 47–49 ps. Now, we expect the prepared fuel to exploit this condition to increase the fusion reaction rate. The results indicate that the breeding ratio is not too sensitive to plasma temperature and choosing 5 keV appears to be a reasonable choice. The correspondence between fuel burning fraction to the initial fuel temperature is presented in figure 8b. We observe a straight line with plasma temperature. But it sweeps a small range.

4. Conclusion

A catalytic mode of DT_x reaction was first studied by Eliezer *et al*. They investigated the fusion reaction of pure D fuel with small T impurity and found the optimum values of initial tritium seed $x = 0.0112$ in central spark ignition. They ignored the effect of hydrodynamic instability in their studies. In this paper, we have shown DT_x fuel burn dynamics in FI method. Such constraints do not appear in FI side. We follow fuel dynamics including external proton beam parameters, energy deposition, hot-spot formation, precompressed fuel heating, all DT fusion reactions and main energy gain–loss term. All these are incorporated in kinematic equations that describe the rate of changes occurring in six species. The coupled equations were solved numerically for the initial fuel configuration assumed in FI. The corresponding final states of burn dynamics were investigated

using the definition of tritium breeding ratio which were observed in detail. It assessed the sensitivity of a given parameter and the corresponding energy gain impact. We have found the proper interval of recommended values for fuel and proton beams. We have summarized this result in table 1.

References

[1] Y Kozaki, *Fusion Eng. Des*. **51**, 1087 (2000)
[2] J D Lindl, R L McCrory and E M Campbell, *Phys. Today* **45**, 32 (1992)
[3] L Feinendegen, E Cronkite and V Bond, *Radiat. Environ. Bioph*. **18**, 157 (1980)
[4] S Eliezer, Z Henis, J Martinez-Val and I Vorobeichik, *Nucl. Fusion* **40**, 195 (2000)
[5] M Mahdavi and B Kaleji, *Plasma Phys. Controlled Fusion* **51**, 085003 (2009)
[6] M H Key, *Phys. Plasmas* **14**, 055502 (2007)
[7] J Meyer-ter-Vehn, *Plasma Phys. Controlled Fusion* **43**, 113 (2001)
[8] X Yang, G H Miley, K A Flippo and H Hora, *Phys. Plasmas* **18**, 032703 (2011)
[9] G R Kumar, *Pramana – J. Phys*. **73**, 113 (2009)
[10] J Pasley, *Pramana – J. Phys.* **75**, 759 (2010)
[11] M Basko, M Churazov and A Aksenov, *Laser Part. Beams* **20**, 411 (2002)
[12] M Temporal, J Honrubia and S Atzeni, *Phys. Plasmas* **15**, 052702 (2008)
[13] J Honrubia, J Fernandez, M Temporal, B Hegelich and J Meyer-ter-Vehn, *Phys. Plasmas* **16**, 102701 (2009)
[14] S Atzeni, *Phys. Plasmas* **6**, 3316 (1999)
[15] M Temporal, R Ramis, J Honrubia and S Atzeni, *Plasma Phys. Controlled Fusion* **51**, 035010 (2009)
[16] S Atzeni and M Ciampi, *Nucl. Fusion* **37**, 1665 (1997)
[17] S Atzeni and M Ciampi, *Fusion Eng. Des.* **44**, 225 (1999
[18] N Luo, M Ragheb and G H Miley, *Fusion Eng. Des.* **85**, 39 (2010)
[19] J Martinez-Val, S Eliezer, Z Henis and M Piera, *Nucl. Fusion* **38**, 1651 (1998)
[20] S Gitomer, R Jones, F Begay, A Ehler, J Kephart and R Kristal, *Phys. Fluids* **29**, 2679 (1986)
[21] J Martinez-Val, S Eliezer and M Piera, *Laser Part. Beams* **12**, 681 (1994)
[22] D Sigmar and G Joyce, *Nucl. Fusion* **11**, 447 (1971)
[23] K Ghosh and S Menon, *Nucl. Fusion* **47**, 1176 (2007)
[24] C K Li and R D Petrasso, *Phys. Rev. Lett.* **70**, 3059 (1993)
[25] T Fukue, H Matsuura and Y Nakao, *J. Plasma Fusion Res.* **8**, 1129 (2009)
[26] F Ognissanto, G Gorini and J Kallne, *Nucl. Instrum. Methods B* **269**, 786 (2011)
[27] O O Beliuskin, V I Grantsev and K K Kisurin, *Probl. Sci. Tech.* **56**, 10 (2011)
[28] J J Devaney, *Nucl. Sci. Eng.* **88** (1984)
[29] J Martinez-Val, *Fusion Tech*. **17**, 476 (1990)
[30] S Eliezer, Z Henis, J Martinez-Val and M Piera, *Phys. Lett. A* **243**, 311 (1998)
[31] M Mahdavi and T Koohrokhi, *Pramana – J. Phys.* **74**, 377 (2010)